Exp.-Nr.: A1/ –98
Eingang:
an PAC:

Mainz Microtron MAMI

Collaboration A1: "Virtual Photons"
Spokesperson: R. Neuhausen

Proposal for an Experiment

First Study of the ^{16}O(e,e$'$np)^{14}N Reaction

Collaborators:

J.R.M. Annand[4], P. Bartsch[3], D. Baumann[3], J. Becker[3], R. Böhm[3], D. Branford[5], S. Derber[3], M. Ding[3], I. Ewald[3], K. Föhl[5], J. Friedrich[3], J.M. Friedrich[3], P. Grabmayr[*1], T. Hehl[1], M. Heim[2], D.G. Ireland[4], P. Jennewein[3], M. Kahrau[3], D. Knödler[2], K.W. Krygier[3], A. Liesenfeld[3], I.J.D. MacGregor[4], H. Merkel[3], K. Merle[3], P. Merle[3], U. Müller[3], H. Müther[2], A. Natter[1], R. Neuhausen[3], Th. Pospischil[3], G. Rosner[*3], H. Schmieden[3], A. Wagner[3], G.J. Wagner[1], Th. Walcher[3], M. Weis[3], S. Wolf[3]

[1] Physikalisches Institut, Universität Tübingen,
[2] Institut für Theoretische Physik, Universität Tübingen,
[3] Institut für Kernphysik, Universität Mainz,
[4] Department of Physics and Astronomy, University of Glasgow,
[5] Physics Department, University of Edinburgh

Contactpersons: P. Grabmayr, Physikalisches Institut, Universität Tübingen
G. Rosner, Institut für Kernphysik, Universität Mainz

Abstract of Physics:

We propose to measure the ^{16}O(e,e$'$np)^{14}N reaction in the same kinematics as the ^{16}O(e,e$'$pp)^{14}C experiment. This first experiment will demonstrate the feasibility of triple coincidence experiments including neutrons with high resolution. The cross sections for *np* and *pp* emission will be used as a first test of recent model predictions and will serve as exploratory study for future investigations of nucleon-nucleon correlations.

Abstract of Equipment:

The two spectrometers B and A will be employed in super-parallel kinematics together with the Tübingen-Glasgow TOF wall (48 bars) and 24 new Veto counters. A waterfilm target will be used.

MAMI–Specifications:

beam energy	855 MeV
beam current	$< 80\ \mu$A
time structure	cw
polarization	none

Experiment–Specifications:

experimental hall	A1 spectrometer hall
beam line	A1
detector	Spectrometer B and A; TOF-wall and Veto-counters

Beam Time Request:

set–up without beam	5 days
set–up with beam	50 hours
data taking	300 hours

Exp.-Nr.: A1/ –98
Eingang:
an PAC:

Mainz Microtron MAMI

Collaboration A1: "Virtual Photons"

Spokesperson: R. Neuhausen

Proposal for an Experiment

16. Nov 1998

First Study of the ^{16}O(e,e$'$np)^{14}N Reaction

Collaborators:

J.R.M. Annand[4], P. Bartsch[3], D. Baumann[3], J. Becker[3], R. Böhm[3], D. Branford[5], S. Derber[3], M. Ding[3], I. Ewald[3], K. Föhl[5], J. Friedrich[3], J.M. Friedrich[3], P. Grabmayr[*1], T. Hehl[1], M. Heim[2], D.G. Ireland[4], P. Jennewein[3], M. Kahrau[3], D. Knödler[2], K.W. Krygier[3], A. Liesenfeld[3], I.J.D. MacGregor[4], H. Merkel[3], K. Merle[3], P. Merle[3], U. Müller[3], H. Müther[2], A. Natter[1], R. Neuhausen[3], Th. Pospischil[3], G. Rosner[*3], H. Schmieden[3], A. Wagner[3], G.J. Wagner[1], Th. Walcher[3], M. Weis[3], S. Wolf[3]

[*] Contact Person
[1] Physikalisches Institut, Universität Tübingen
[2] Institut für Theoretische Physik, Universität Tübingen
[3] Institut für Kernphysik, Universität Mainz
[4] Department of Physics and Astronomy, University of Glasgow
[5] Physics Department, University of Edinburgh

Abstract

We propose to measure the ^{16}O(e,e$'$np)^{14}N reaction in order to study for the first time the virtual photon induced emission of neutron-proton pairs from an atomic nucleus with sufficient resolution to separate the final states. This investigation will result in information complementary to those obtained from previous studies of (γ,NN) and (e,e$'$pp) reactions. For comparison of cross sections in the *np* and *pp* channels the kinematical setting will be the same as it was for the recent, high-resolution ^{16}O(e,e$'$pp) experiment. The focus of the present ^{16}O(e,e$'$np) experiment will be on the ground state transition to ^{14}N, because this involves the emission of an $T = 0$, $S = 1$ np-pair where tensor correlations can contribute – a subject of upcoming studies.

1 Introduction

This proposal follows along our line of research on nucleon-nucleon (NN) correlations in atomic nuclei. The concept of correlations was introduced to account for deviations from the mean field behaviour of nucleon pairs inside the nuclear medium. In particular, the NN forces at short distances, i.e. the central, repulsive part of the interaction below 0.5 fm and the tensor forces, which dominate the NN potential for $T = 0$, $S = 1$ pairs at slightly larger distances play an important rôle for the binding of the nucleus. As the mean field behaviour is mainly determined by the long-range part of the NN potential, effects of NN correlations remained vastly hidden in the past. Consequently, Hartree-Fock approaches had to use effective, purely phenomenological NN potentials to yield bound nuclei.

Therefore, correlations can only be made evident via the detailed comparison of appropriate experiments with elaborate models. They have to describe the NN dynamics accurately using realistic potentials and have to account for competing reaction mechanisms as well as final state interaction. In particular it is noted that the data sets have to comprehend information on all the reaction channels to permit a proper treatment of the disturbing effects of FSI.

The determination of occupancies of shell model orbitals was one of many approaches and studies towards NN correlations in the last decade. In hadronic and electromagnetic one-nucleon knockout and transfer reactions the spectroscopic amplitudes have been studied. However, in retrospective only relative strengths could be extracted, mostly because of distortions of incoming and outgoing particles. One approach — almost free of impeding assumptions — constituted the CERES method [1], which obtained the occupancy of the $3s_{1/2}$ orbits from combining density distributions from electron scattering data with relative spectroscopic factors. The determined occupancy of $\approx 75\%$ showed the existence of NN correlations in addition to long-range RPA-type correlations in accordance with variational calculations [2]. However, it was beyond this method's power to reveal any detailed information.

Thus, our research was tuned towards two-nucleon emission induced by electromagnetic probes. The basic idea of this approach had been formulated by Gottfried [3] in the fifties. Relying on simplifying assumptions Gottfried wrote the cross section for photon-induced 2N emission as a product of a kinematical part depending on the momentum P of the nucleon pair and a matrix element S_{fi} depending on the relative momentum distribution p_{rel}

$$d\sigma \sim F(P) \cdot S_{fi}(p_{rel})$$

The latter contribution contains the two-body dynamics and therefore is of particular interest. The transverse nature of real photons makes them an ideal tool for studies of two-body currents. Therefore the (γ,np) reactions are dominated by (charged) meson exchange currents (MEC)and Isobar Currents (IC). The (γ,pp) channel would be a better candidate for the study of correlations than (γ,np), insofar as MEC and Δ resonance contributions are greatly reduced [4]. On the other hand, final state interactions (FSI) come into play when flux from the much stronger (γ,np) channel "pollutes" the weak *pp* channel via FSI. Furthermore, as discussed later, the important tensor correlations are accessible in the *np* channel only.

To interpret the (γ,NN) reactions, to quantify the various contributions and establish regions where the photoabsorption on two nucleons dominates, the Valencia model [5] has been used, which microscopically calculates the photon absorption cross sections using a Fermi-gas model and a local density approximation. However, the knocked on nucleons and produced pions are tracked through the nucleus just via a semi-classical method. We have adapted this model to include the exact experimental kinematical conditions for a realistic comparison [6]. Fig. 1

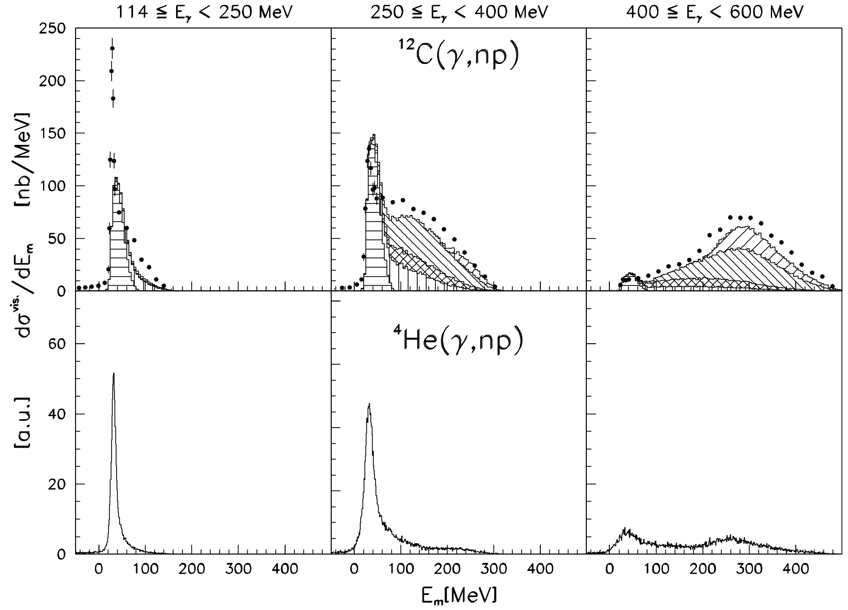

Figure 1: Missing energy spectra for the (γ,np) reaction on the nuclei ^{12}C (top row, ref. [6]) and ^{4}He (bottom row, ref. [7]) for three different photon energy bins. The ^{12}C data are compared to results from the Valencia model [5]. The different reaction mechanisms are indicated by the hatching. $\boxed{-}$ direct NN absorption, $\boxed{|\,|}$ NN absorption + FSI, $\boxed{\times}$ 3N absorption (+FSI), $\boxed{\backslash}$ + $\boxed{/}$ pion production with and without reabsorption, respectively

shows the level of agreement reached for the ^{12}C(γ,np) reaction at three different photon energy ranges. The different reaction mechanisms are indicated by different hatching of the areas. The following is noted: a) the overall agreement between calculations and the data is satisfying; b) a comparison of the ^{12}C data to the ^{4}He data, shown in the lower panel of this figure, demonstrates the reduction of final state interaction with reduced target mass. However, the two residual nucleons are in the continuum in contrast to real nuclei, where the quantum numbers of resolved final states can be used for a reduction of contributing final states; c) the dominance of two-nucleon absorption at low excitation energy of the final nucleus or equivalently at low missing energies E_{2m} (=$E_\gamma - T_p - T_n - T_R$) can clearly be seen at all photon energies. As can be seen from Fig. 1, FSI does not play a major role in this low-energy regime. This is contrary to the much weaker (γ,pp) channel where contributions due to FSI exhaust a large fraction of cross section which might be the cause for poor agreement with model predictions [6, 8]. From these results it is concluded that one has to concentrate on low missing energies for more detailed studies of NN correlations. For low lying states other models [10, 11] which treat the nuclear structure in more detail can be used. However, these models neglect and/or approximate some of the competing mechanisms and therefore do not permit to extend the interpretation towards higher photon energies. The recent calculations [10, 11] do not invoke the closure approximation anymore, rather they predict cross sections for transitions to individual final states. In particular, the potential of resolved final states for scrutinising tests of contributing partial waves is emphasised. Therefore, our efforts concentrate on improving the experimental resolution.

Another observable which is closely related to NN-correlations is the relative momentum $\vec{p}_{rel} = (\vec{p}_p - \vec{p}_n)/2$ between the two nucleons involved. For p_{rel} above 200 MeV/c relative distances below 1 fm are probed. Results of distributions measured with real photons are shown

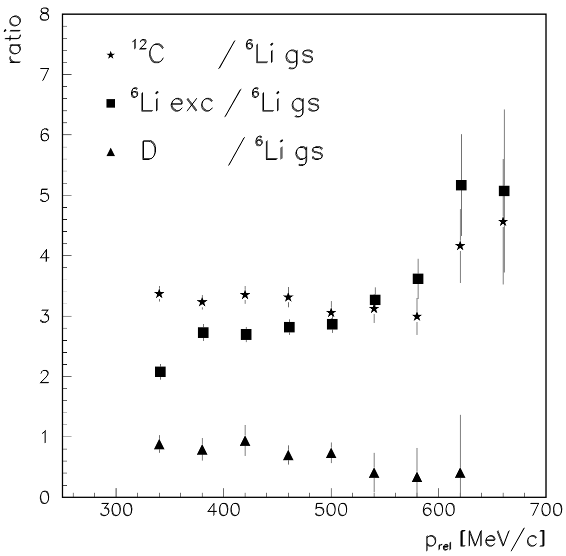

Figure 2: Relative momentum distributions for the (γ,np) reaction on D, ^{12}C and ^{6}Li normalised to those obtained with good statistics from the ^{6}Li(γ,np)^{4}He g.s. reaction which was shown [12] to be equivalent to that of the deuteron disintegration [14].

in Fig. 2. In order to avoid model-dependent discussions we do not show absolute distributions but those normalised to the free *np* pair, the deuteron. Unfortunately, the statistical accuracy in the Deuterium runs was not high enough and therefore the data obtained for the ^{6}Li(γ,np)^{4}He g.s. reaction was used for normalisation instead. However, it has been shown earlier that these two distributions are equivalent [12]. The results of Fig. 2 show a flat distribution up to relative momenta of about 500 MeV/c, slightly rising afterwards [9, 13, 14]. These preliminary results are taken as hints of the existence of NN correlations. It is obvious that correlation effects are most apparent at high values of p_{rel}.

It should be emphasised that in order to reach these results, it was necessary to cover a large range in phase space which was achieved by use of two detector systems of 1 sr solid angle each. This enabled a rather useful variation of the various observables for the necessary study of the competing reaction mechanisms as well as for the correlations themselves.

Virtual photons in contrast to real photons carry longitudinal polarisation as well. The longitudinal cross section is dominated by one-body currents and is therefore very sensitive to short-range correlations (SRC) and moreover, less affected by IC and by MEC. First (e,e$'$pp) experiments on ^{12}C [15] and ^{16}O [16, 17] have been performed, the latter with an energy resolution of $\Delta E_{2m} < 0.5$ MeV. Individual states could be resolved, which in turn show different pair momentum distributions, depending on the spin of the observed states. It is understood that a quantitative comparison with theory will restrict the choice of potentials and thus shed light on the nature of NN correlations at short internucleon distances [18]. However, the question arises how clean the *pp* channel actually is, i.e. how much strength is shifted by FSI from the strong *np* channels into the *pp* channel. To approach this question the (e,e$'$np) reaction has to be measured permitting first comparisons with model calculations.

There is experience with real photons about the relative importance of knockout of *np* and *pp* pairs [6, 8, 12, 19]. To illustrate this fact the photon energy dependence of the cross sections for the ^{12}C(γ,np) and ^{12}C(γ,pp) is shown in Fig. 3 for two regions of low missing energy

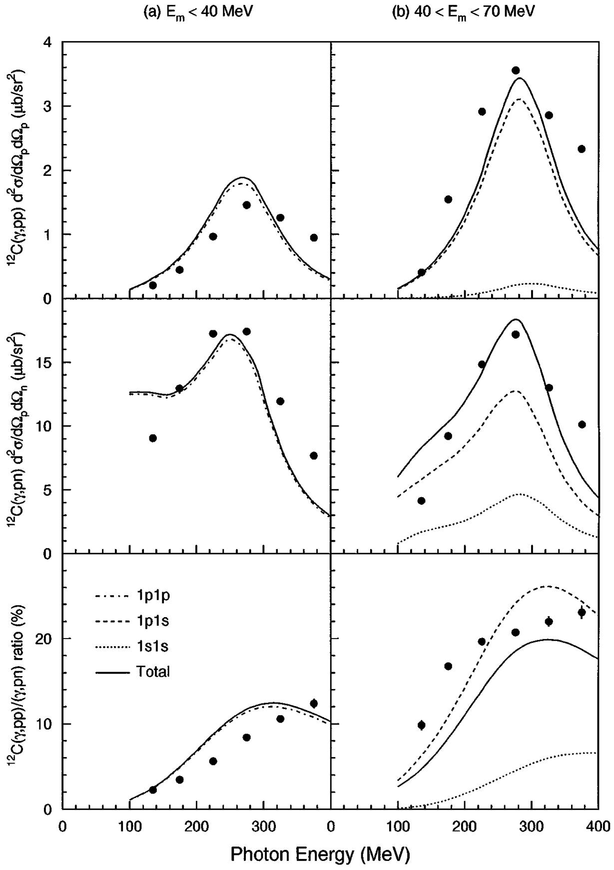

Figure 3: Excitation function for the (γ,pp) and (γ,np) reactions on ^{12}C for two ranges of missing energy [19]; (a) E_{2m} <40 MeV, (b) 40 < E_{2m} < 70 MeV. The bottom two panels give the photon energy dependence of the cross section ratio (γ,np)/(γ,pp).

together with their ratio [19]. Due to the transverse nature of real photons the Δ resonance is a dominant feature in both channels. Apart from the absolute sizes which differ by an order of magnitude mostly through the contributions by MEC, there are minor differences in shape or in the angular distributions (see refs. [6, 19]). The *np*/*pp* ratio varies from ≈ 5 to 20. Without proper modeling an excess in the (γ,pp) cross section might be easily misinterpreted. The relevance of these findings with real photons for the case of virtual photon induced reactions arises from the fact that even in optimised kinematics the transverse cross section remains quite large. Measurements have to verify the model calculations in selected kinematics which has not been done so far for a nuclear target.

2 Knockout of *pp* and *np* pairs

A ^{16}O(e,e′pp)^{14}N experiment [17] has been performed with a missing energy resolution of $\Delta E = 0.5$ MeV and thus resolving the dominant 2 hole-states in ^{14}C. The cross sections are described well by model calculations of the Pavia group using correlation functions based on the G-matrix approach to nuclear matter [18]. Therefore, taking the kinematics for the proposed ^{16}O(e,e′np) experiment is a natural choice for the comparison of cross sections and reaction mechanisms for *pp* and *np* emission. This exploratory experiment should also demonstrate that

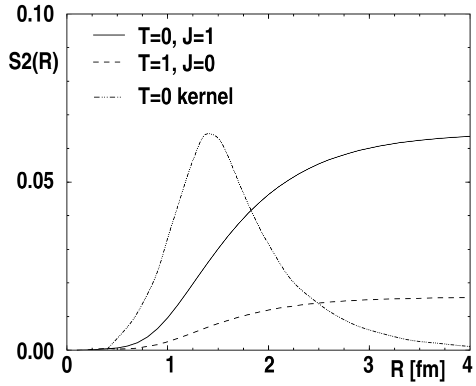

Figure 4: Results for the Wound integral as defined in eq. 1 [20].

the neutron arm reaches sufficient resolution warranting more extensive investigations. ^{16}O is the best choice as a nuclear target because of its closed shell nature and the large level spacing of the residual nuclei ^{14}C and ^{14}N. In addition, work with real and virtual photons has already been started. Furthermore, also theoretical investigations have concentrated on ^{16}O.

In this context we wish to discuss the relative strength of *np* and *pp* correlations and their contribution to the total cross section. Interest in the (e,e′np) reaction arises through the tensor correlations which for s-waves are completely absent in the *pp* channel. Central, short range correlations contribute to both channels. The unique access to this type of NN correlations makes the (e,e′np) reaction an attractive tool, despite the impeding fact of an increase in MEC. Sofar tensor correlations have been theoretically studied in a consistent treatment together with MEC and IC only in nuclear matter [21]. First calculations for finite nuclei are underway [22, 23]. It is generally believed that the relative importance of the various contributions, i.e. MEC, IC and correlations as calculated in nuclear matter, does not change much in nuclei, e.g. ^{16}O. In the discussion below we will show that the influence of NN correlations in the *np* channel exists in particular in the longitudinal part and in the transverse cross section at high photon momentum (at fixed energy transfer). The super-parallel kinematics reduces IC and MEC contributions also in the case of *np* pair emission, as was shown for $(e, e'pp)$ reactions in [15].

First, the effects of correlations in $T = 0$ and $T = 1$ pairs is demonstrated in Fig. 4 where the two-body correlation function $S2(R)$ is plotted as a function of the upper limit R of the integration variable r, the relative inter-nucleon distance.

$$\begin{aligned} S2(R) &= \sum_\alpha \int_0^R dr\, r^2 \,|< r, \alpha|S2|p_{1/2}p_{1/2}JT > |^2 \\ &= \int_0^R dr\, r^2 \,| < \Psi_{A-2}|\Psi_A > - < \Phi_{A-2}|\Phi_A >|^2 \end{aligned} \tag{1}$$

where Ψ and Φ are the correlated and Hartree-Fock (uncorrelated) wave functions of nuclei A and $(A-2)$, respectively. The overlap integral constitutes the two-body densities and consequently the so called Wound integral S2(∞) which is a very good measure for two-body effects taking into account the interaction volume. The present example is given for two nucleons in ^{16}O from the $p_{1/2}$ orbital coupled to total angular momentum $S = 1$ (resp. 0) and isospin $T = 0$ (resp. 1). The Argonne V14 [24] potential has been used to calculate the NN interaction summed over all partial waves α. It is noted, that at all relative distances r the correlation effects for the $T = 0$ pair are a factor of 4 larger than those for the $T = 1$ case. The kernel (dot-dashed line) of the $T = 0$ integral demonstrates clearly that the dominant contributions arise when the two active nucleons have a distance of 1-2 fm from each other, which holds true also for $T = 1$ pairs.

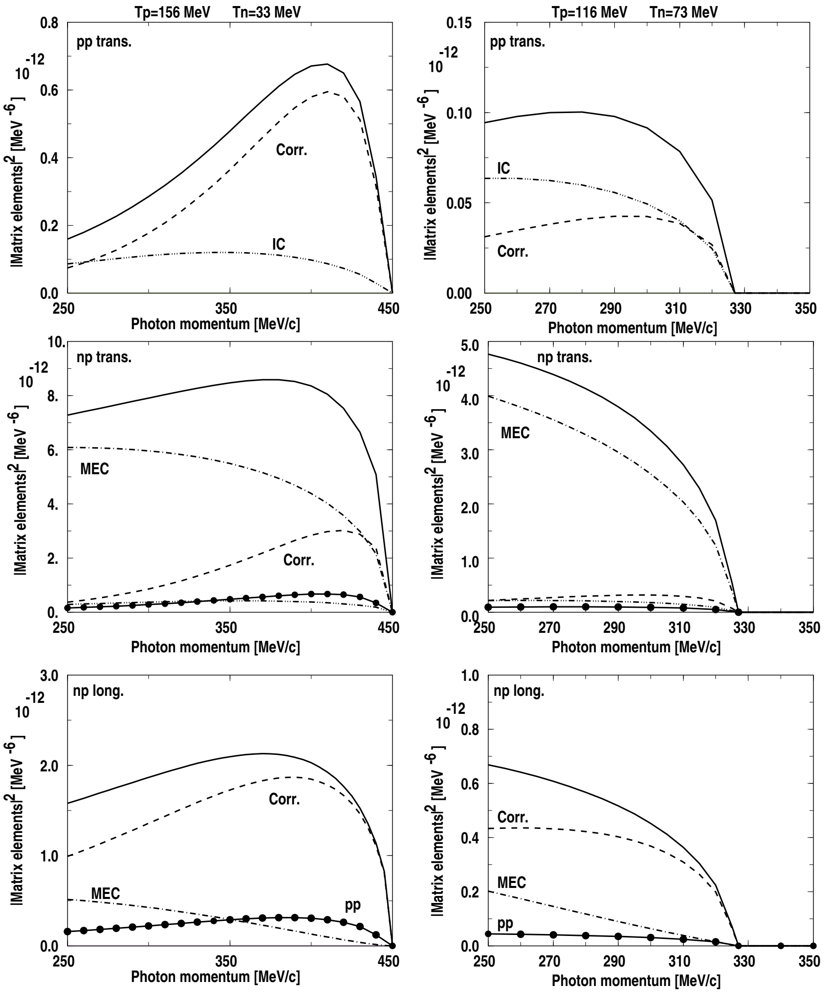

Figure 5: Matrix elements squared of the (e,e′np) and (e,e′pp) reaction are split into contributions from correlations (Corr.), meson exchange currents (MEC) and Δ contributions (IC) for a typical super-parallel kinematical setup with ω=215 MeV and fixed nucleon energies (left,right column) as given on top of each column.

First theoretical investigations for *np* emission have been made [21] in order to locate those kinematics where correlations are most prominent. As an example of results, the matrix elements squared are shown in Fig. 5 as a function of the photon momentum $\mid \vec{q} \mid$ for fixed energy transfer ω=215 MeV. These calculations are performed assuming super-parallel kinematics when a fast proton is emitted forward, parallel to $\vec{q}$ and a neutron with low kinetic energy in anti-parallel direction. As in the (e,e′pp) reaction this kinematic suppresses the unwanted contributions from IC and MEC. From Fig. 5 it is evident that correlations gain importance at high photon momentum.

Preliminary calculations including correlations [20] as obtained for finite nuclei as well as the reaction model [18] used for (e,e′pp) are getting available at this moment. A comparison for ^{16}O(e,e′NN) leading to the ground states in the residual nuclei and the isobaric analog are given in Fig. 6. They show the expected excess of *np* yield over the *pp* yield. For the isobaric analog state in ^{14}N the *np* pair is in a $T = 1$ state, therefore already MEC alone cause an increase by a factor of 5. For the ground state transition the cross sections are bigger by roughly another factor of 4.

States of interest in ^{14}N are compiled in table 1.

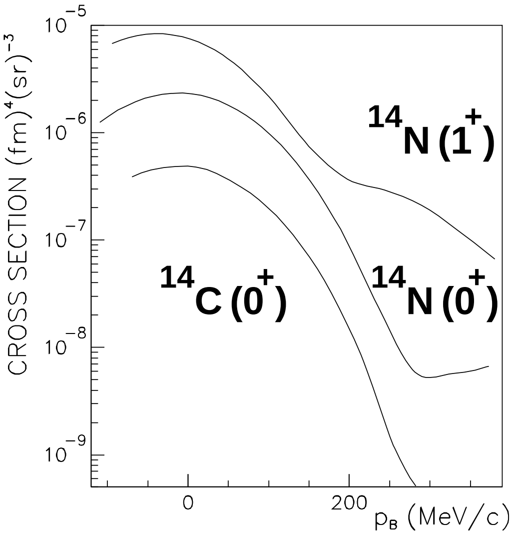

Figure 6: First calculations [18, 20, 23] of the recoil momentum ($p_B = p_{2m}$) distributions for the (e,e′np) and (e,e′pp) reactions on ^{16}O leading to discrete final states in ^{14}N and ^{14}C (k=855 MeV; ω=215 MeV/c; q=316 MeV). Note, that the ^{14}N,0$^+$ (first excited state, $T = 1$) is the isobaric analog state to the ^{14}C,0$^+$ (ground state, $T = 0$)

Table 1: Low-lying states in ^{14}N.

E_x/MeV	J^π_R, T	configuration	L
0.00	1^+,0	$(p_{1/2})^{-2}$	2
2.30	0^+,1	$(p_{1/2})^{-2}$	0
3.95	1^+,0	$(p_{1/2})^{-1}(p_{3/2})^{-1}$	0
7.03	2^+,0	$(p_{1/2})^{-1}(p_{3/2})^{-1}$	2
11.05	3^+,0	$(p_{3/2})^{-2}$	2

The present status of knowledge suggests the following specifications for the ^{16}O(e,e′np) experiment:

a) choice of kinematics with large longitudinal photon polarisation (ε_L=0.91).

b) energy transfer below $\omega = 250$ MeV to reduce Δ resonance contributions ($\omega = 215$ MeV).

c) detection of the proton in parallel kinematics to remove interference structure functions.

d) resolve final states in order to exploit the state dependences of the various contributions.

e) studies of the (e,e′NN) reaction mechanisms:

  - Coverage of the neutron emission angle around super-parallel kinematics in order to select the optimal kinematical region, i.e. neutron in "anti-$\vec{q}$" direction to reduce Δ resonance contributions. The minimum in cross sections at anti-parallel emission angle will be verified.
  - Detection of protons in backward direction simultaneously to the neutrons in order to study the relative strength in the (e,e′pp) and (e,e′np) reactions.

3 Experimental setup

The proposed ^{16}O(e,e′np) experiment will be performed in the 3-spectrometer hall of the MAMI facility relying mostly on existing components to be put together for the first time in the suggested configuration. Part of the work needed here is essential also for the planned ^{3}He(e,e′np) experiment. For ease of comparison the kinematical setting of this first ^{16}O(e,e′np) experiment will be as close as possible to the ^{16}O(e,e′pp) reaction already under investigation.

3.1 Kinematics

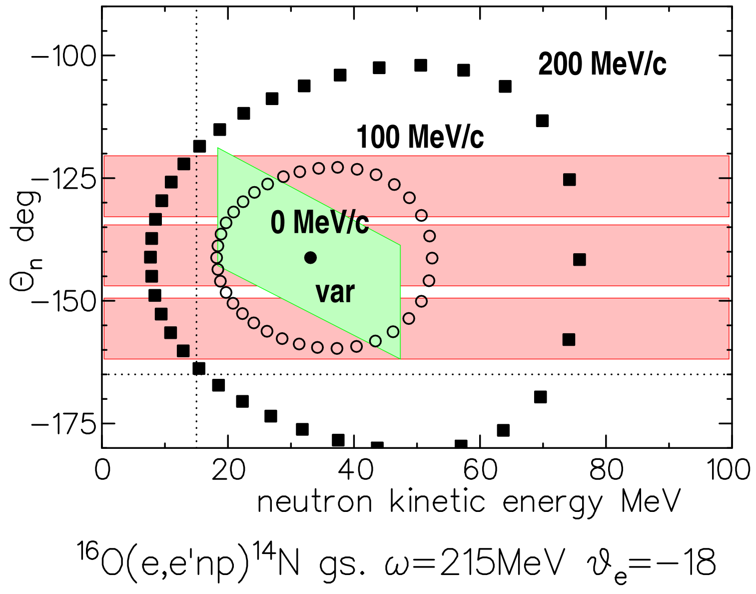

Figure 7: Dependence of neutron kinetic energy and emission angle as function of missing momentum p_{2m} for fixed proton angle and electron kinematics. Three missing momenta have been assumed. The three horizontal areas indicate the position of the neutron detectors whereas the diamond shaped area is indicative of the acceptances of the spectrometers A and B (assumed p_{2m}=0 MeV/c). The dotted lines show the constraints due to thresholds and geometry.

The kinematics suggested by physics is also favourable from the experimental point of view. The fast forward going proton can easily be picked up from the large electromagnetic background via a magnetic spectrometer. The background rates are relatively low permitting the detection of slow backward going neutrons with scintillation counters still gaining good energy resolution. The total energy resolution is limited by the neutron contribution because of the high resolution of the two spectrometers used for protons and electrons. The kinematical situation is exemplified in Fig. 7 where the neutron kinetic energy and polar emission angle are shown for a fixed momentum transfer and a proton angle as defined by the central values of the two spectrometers A and B. The angular range covered by the three frames of TOF detectors is indicated by the three hatched areas and the acceptance limits by the dotted lines. For a nucleon pair at rest the kinematics results in a single pair of neutron energy and angle. The variation due to the finite acceptances of the magnetic spectrometers is indicated by the diamond shaped area effectively enlarging the accessible range. Variation of initial pair momenta results in a variation of the final nucleon energies and neutron angles (note, that the proton angle remains fixed): two egg-shaped rings in Fig. 7 represent the central values of the spectrometer acceptances. Acceptance variation would produce similar diamond shaped regions for each entry. Thus, the spectrometer acceptance makes accessible a larger kinematical range demonstrating the large acceptance of the complete setup. When selecting a missing momentum of 100 MeV/c the proton kinetic energies (momenta) vary between 140 (531) and 174 MeV (600 MeV/c).

3.2 Target

The Mainz waterfilm target will be used. It has a thickness of 50 mg/cm^2.

3.3 Electron spectrometer

Spectrometer B [26] of the 3-spectrometer hall will be used for the momentum determination of the scattered electron. The main characteristics are a solid angle $\Delta\Omega$ = 5.6 msr, a momentum acceptance $\Delta p/p$ = 15% and a resolution of $\delta p/p \approx 10^{-4}$. The suggested kinematics requires a scattering angle of θ_e = -18 ° and a central electron momentum $\overline{k'}$ = 640 MeV/c corresponding to ω=215 MeV in order to stay well below the Δ resonance. From this a mean momentum transfer of $|\vec{q}\,|$ = 316 MeV/c results as well as an angle of $\theta_q = 38°$ with respect to the beam. The virtual photon polarisation amounts to $\varepsilon_L = 0.91$.

3.4 Proton spectrometer

Spectrometer A [26] of the 3-spectrometer hall will be setup to accept the fast forward going protons. Its main characteristics are a solid angle $\Delta\Omega$ = 28 msr, a momentum acceptance $\Delta p/p$ = 20% and a resolution of $\delta p/p \approx 10^{-4}$. The super-parallel kinematics requires a proton detection angle of $\theta_p = 38°$ ($=\theta_q$) and two settings of central proton momentum to cover the missing momentum p_{2m} range of $-100 < p_{2m} < 200$ MeV/c.

3.5 Neutron TOF detectors

The Tübingen-Glasgow time-of-flight detectors [27] will be equipped with new veto counters immediately in front of the TOF bars. This differs from setups with real photons performed in the tagger hall. This modification is necessary due to the high electron flux and background close to the target area. The TOF bars will be positioned at a distance of 8 m from the target where one frame covers an angular range of $\Delta\theta_n$=12°. All three of them will span the θ_n range from -120° to -165° centred around the anti-parallel direction ($\theta_q + 180°$).

The 3 cm uncertainty in the (on average) 8 m long flight path arises mainly through the thickness of the scintillator bars. Assuming timing resolutions of 0.5 and/or 0.7 ns (FWHM) for the neutron and electron arm (stop and start time resolution) the overall neutron energy resolution is calculated (Fig. 9). For the major part of the neutrons of interest a resolution better than ΔE_n = 1.4 MeV (FWHM) was found. Because the combined contribution from the electron and proton is estimated to be 0.5 MeV, this neutron resolution suffices to obtain a

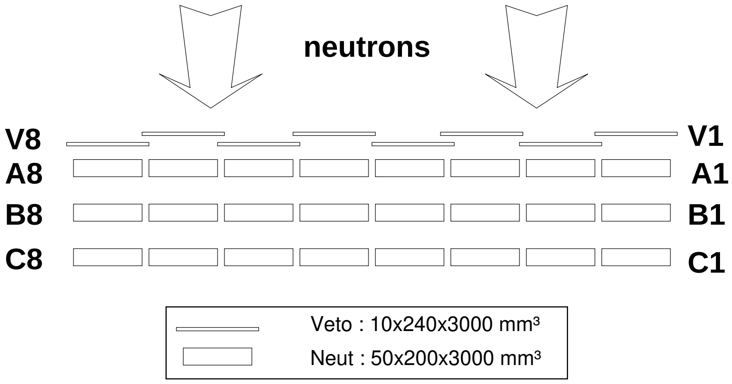

Figure 8: Horizontal cross section through one stand of TOFs holding one layer of 8 veto counters (V) and three layers of 8 TOF bars (A-C) each. Three stands in total will be employed.

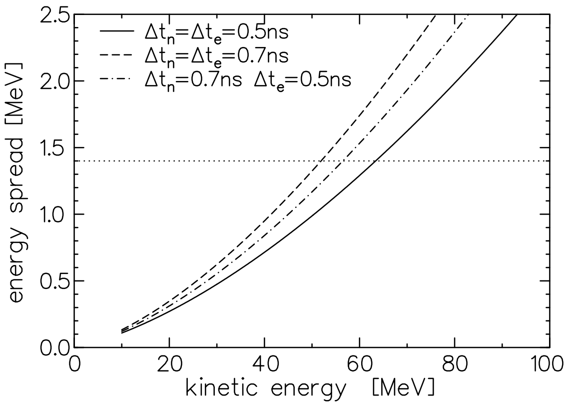

Figure 9: TOF energy resolution as function of neutron kinetic energy for three pairs of timing resolutions.

total energy resolution of better than 1.5 MeV which permits the separation of the transition to the ground state in ^{14}N.

The neutron detection efficiency is about 5% per TOF bar. Three layers increase the neutron efficiency to $\approx$ 15%. Detailed simulations are under way.

The front-end electronics will be located close to the neutron detectors and connections between the TOF and spectrometer sub-triggers will be done in the spectrometer hall in order to avoid any unnecessary delay.

Thresholds will have to be set carefully to the effect that any charged particle will make a signal in the veto counters. However, the veto function will be applied only offline in order to enable the simultaneous registration of protons and neutrons in the TOF array. This technique has been applied successfully for the (γ,np) and (γ,pp) experiments in the tagger hall.

3.6 Tests

A first test of count rates has been performed in the spectrometer hall for neutron detector positions similar to the ones suggested here [28]. Singles count rates of less than 0.4 MHz have been observed at luminosities up to $\mathcal{L} = 1.4\cdot 10^{37}$ nucleons/(s·cm^2) (^{12}C of 45 mg·cm^{-2} @ 80 μA). These results have encouraged to propose the present (e,e′np) experiment.

The new veto counters have to be setup and tested in the 3-spectrometer hall. Furthermore, the trigger and triple coincidence circuitry has to be realised and checked.

4 Beam time request

On average, the same count rates are expected in ^{16}O(e,e′np) as compared to (e,e′pp) experiments as the increase in cross section for the np-channel is counterbalanced by a ≈15% neutron detection efficiency.

The cross section for the ^{16}O(e,e′pp)^{14}C ground state transition was measured to σ_{pp}= 250 fb/(MeV^2·sr^3). From Fig. 6 one deduces an increase in cross section for the ^{16}O(e,e′np)^{14}N ground state transition by a factor 20, i.e. we assume σ_{np}=5 pb/(MeV^2·sr^3) for the count rate estimate at $p_{2m} \approx 0$ MeV/c. With

- solid angle of electron spectrometer $\Delta\Omega_e$ = 5.6 msr
- solid angle of proton spectrometer $\Delta\Omega_p$ = 28 msr
- solid angle of TOF array $\Delta\Omega_n$ = 3 × 66 msr = 200 msr
- neutron detection efficiency (3 layers) $\epsilon = 0.15$
- target density n_T = 50 mg/cm^2 = $1.7 \cdot 10^{21}$ nuclei/cm^2
- electron current I = 75 μA = $4.9 \cdot 10^{14}$ s^{-1}

the count rate N for the ground state transition is estimated according

$$N = I\ n_T\ \epsilon\ \sigma_{np}\ \Delta\Omega_e\ \Delta\Omega_p\ \Delta\Omega_n \tag{2}$$

to N ≈1 counts per hour and per 10 MeV/c of missing momentum. The rate for the transition to the analog state amounts to ≈0.2 counts per hour and per 10 MeV/c of missing momentum. At a missing momentum of p_{2m} ≈200 MeV/c the cross sections have decreased by about an order of magnitude. With two magnetic field settings of the proton spectrometer a missing momentum distribution in the range -100 < p_{2m} < 200 MeV/c with a binning of 60 MeV/c and with statistical uncertainty better than 15% could be achieved within a beam time of 300 hours.

Table 2: beam time request

beam time	300 hours
setup time	50 hours

The setup time (with and without beam) will be shared with the ^{3}He setup whenever possible.

References

[1] P. Grabmayr, Prog. Part. Nucl. Phys. **29** (1992) 251

[2] V.J. Pandharipande *et al.*, Rev. Mod. Phys. **59** (1997) 981

[3] K. Gottfried, Nucl. Phys. **5** (1958) 557

[4] J. Ryckebusch *et al.*, Nucl. Phys **A568** (1994) 828

[5] R.C. Carrasco, M.J. Vicente-Vacas und E. Oset, Nucl. Phys. **A570** (1994) 801

[6] Th. Lamparter *et al.*, Z. Phys. **A 355**(1996) 1

[7] F.A. Natter, PhD thesis, U. Tübingen, in preparation

[8] P.D. Harty *et al.*, Phys. Rev. **C57** (1998) 123

[9] P. Grabmayr, in "Correlations and Clustering Phenomena in subatomic physics", eds. M.N. Harakeh, J.H. Koch and O. Scholten: NATO ASI Physics 359, p. 53, 1996, Plenum Press

[10] S. Boffi *et al.*, Nucl. Phys. **A564** (1993) 473

[11] J. Ryckebusch *et al.*, Nucl. Phys. **A624** (1997) 581

[12] P. Grabmayr *et al.*, Phys. Lett. **B370** (1996) 17

[13] P. Grabmayr *et al.*, contrib. to Proc. of the XIV PANIC, Williamsburg 1996, World Scientific, 1997

[14] T. Lamparter, PhD thesis, U. Tübingen, 1997

[15] K.I. Blomqvist *et al.*, Phys. Lett. **B421** (1998) 71

[16] C.J.G. Onderwater *et al.*, Phys. Rev. Lett. **78** (1997) 4893

[17] G. Rosner, Proc. on "Perspectives in Hadron Physics", eds. S.Boffi, C. Ciofi degli Atti und M. Giannini, p. 185, World Scientific 1998

[18] C. Giusti *et al.*, Phys. Rev. **C57** (1998) 1691

[19] I.J.D MacGregor *et al.*, Phys. Rev. Lett. **80** (1998) 245

[20] H. Müther, priv. communication

[21] D. Knödler, PhD thesis, U. Tübingen, in preparation

[22] M. Heim, PhD thesis, Tübingen, in preparation

[23] C. Giusti, priv. communication

[24] R.B. Wiringa, R.A. Smith und T.L. Ainsworth, Phys. Rev. **C29** (1984) 1207

[25] W.J.W. Geurts, K. Allaart, W.H. Dickhoff und H. Müther, Phys. Rev. **C54** (1996) 1144

[26] K.I. Blomqvist *et al.*, Nucl. Instr. Methods **A403** (1998) 263

[27] P. Grabmayr *et al.*, Nucl. Instr. Methods **A402** (1998) 85

[28] P. Grabmayr, Internal Report IR97/5, Physikalisches Institut, Tübingen 1997